Sheetz, M. P., & Singer, S. J. (1974) *Proc. Natl. Acad. Sci. U.S.A. 71*, 4457–4461.
Stockton, G. W., Polnaszek, C. F., Leitch, L. C., Tulloch, A. P., & Smith, I. C. P. (1974) *Biochem. Biophys. Res. Commun. 60*, 844–850.
White, J. G. (1974) *Am. J. Pathol. 77*, 507–518.
Wintrobe, M. M. (1981) *Clinical Hematology*, 8th ed., Lea & Febiger, Philadelphia, PA.
Zlatkis, A., Zak, B., & Boyle, A. J. (1953) *J. Lab. Clin. Med. 41*, 486–492.

Lipid Transfer between Phosphatidylcholine Vesicles and Human Erythrocytes: Exponential Decrease in Rate with Increasing Acyl Chain Length†

James E. Ferrell, Jr., Kong-Joo Lee, and Wray H. Huestis*
Department of Chemistry, Stanford University, Stanford, California 94305
Received June 18, 1984; Revised Manuscript Received November 6, 1984

ABSTRACT: The rate of phospholipid transfer from sonicated phospholipid vesicles to human erythrocytes has been studied as a function of membrane concentration and lipid acyl chain composition. Phospholipid transfer exhibits saturable first-order kinetics with respect to both cell and vesicle membrane concentrations. This kinetic behavior is consistent either with transfer during transient contact between cell and vesicle surfaces (but only if the fraction of the cell surface susceptible to such interaction is small) or with transfer of monomers through the aqueous phase. The acyl chain composition of the transferred phospholipid affects the transfer kinetics profoundly; for homologous saturated phosphatidylcholines, the rate of transfer decreases exponentially with increasing acyl chain length. This behavior is consistent with passage of phospholipid monomers through a polar phase, which might be the bulk aqueous phase (as in the monomer transfer model) or the hydrated head-group regions of a cell–vesicle complex (transient collision model). Collisional transfer also predicts that intercell transfer of phospholipids should be slow compared to cell–vesicle transfer, as surface charge and steric effects should prevent close apposition of donor and acceptor membranes. This is not found; dilauroylphosphatidylcholine transfers rapidly between red cells. Thus, the observed relationship between acyl chain length and intermembrane phospholipid transfer rates likely reflects the energetics of monomer transfer through the aqueous phase.

In the preceding paper (Ferrell et al., 1985), phospholipid transfer from synthetic vesicles to human erythrocytes served as a convenient method for changing the bilayer balance of the erythrocyte membrane. However, lipid transfer is a phenomenon of broader theoretical and practical interest, being of central importance for an understanding of membrane lipid dynamics.

Two types of mechanisms have been proposed for the spontaneous transfer of lipids between biological membranes (Figure 1). The first involves lipid transfer during transient collisions between the donor and acceptor membranes. In the second, lipid monomers dissociate from the donor membrane, diffuse through the aqueous phase, and associate with the acceptor membrane. Evidence from several laboratories favors the second model for the transfer of phospholipids and cholesterol between a variety of donors and acceptors (Martin & MacDonald, 1976; Duckwitz-Peterlein et al., 1977; Roseman & Thompson, 1980; Nichols & Pagano, 1981; Backer & Dawidowicz, 1981; McLean & Phillips, 1981; Massey et al., 1982; DeCuyper et al., 1983; Lange et al., 1983), although other evidence supports the collision model (Martin & MacDonald, 1976; Kremer et al., 1977).

It is frequently argued that the kinetics of lipid transfer can distinguish between these two models, supposing the rate of transfer to be first order in both donor and acceptor membrane concentrations in the collision model and first order in donor concentration alone in the monomer transfer model. As the following discussion will show, this distinction is valid only for limiting cases. In general, initial transfer rates depend on donor and acceptor concentrations in a saturable (hyperbolic) fashion in both models. The kinetic data that have been garnered in support of monomer transfer do not rule out the transient collision model.

Given this ambiguity, further tests are required to distinguish between the two models. The collision model can be evaluated by altering the physical properties of the donor and acceptor membranes in ways that discourage formation of complexes. The monomer transfer model can be tested by examining a prediction which follows from simple thermodynamic arguments. The dissociation of a lipid monomer into the aqueous phase would increase the ordering of the water molecules that contact its acyl chains. The free energy of this process should be directly proportional to the length of the chains (Tanford, 1980). The Hammond postulate (March, 1977) predicts that the transition state of a dissociating lipid would resemble a free monomer. Thus, the free energy of activation would also be roughly proportional to the length of the acyl chains, and the rate of lipid transfer would decrease sharply as acyl chain length increased. In particular, the rate coefficient for monomer dissociation (k_1 in Figure 1c) would decrease exponentially with increasing chain length. In the present study, we measured the kinetics of transfer of five

† This work was supported by grants from the National Institutes of Health (HL 23787) and the American Heart Association (Grant in Aid 80990).

0006-2960/85/0424-2857$01.50/0

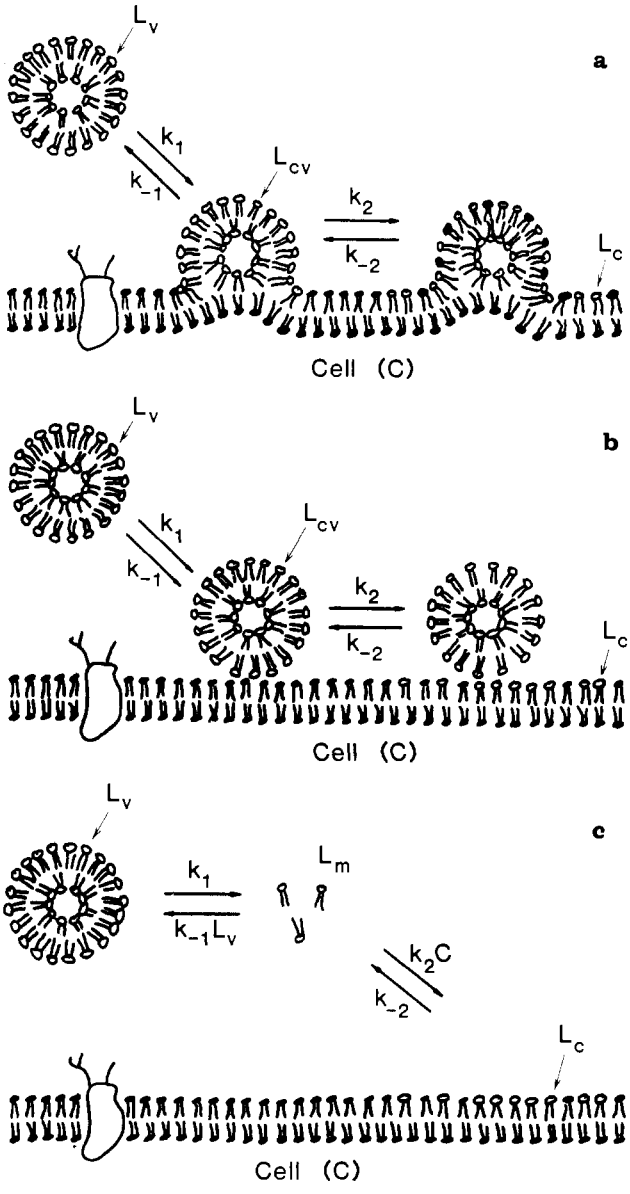

FIGURE 1: Schematic representation of (a and b) transient collision and (c) monomer transfer models. In (a), the lipid transfer step involves lateral diffusion of lipids between partially fused cell–vesicle complexes. In (b), lipid transfer occurs as a result of interbilayer translocation or flip-flop within the cell–vesicle complex. Abbreviations: L_v, vesicle lipid; C, cells; L_{cv}, lipid in cell–vesicle collision complexes; L_c, lipid incorporated into the cells; L_m, monomeric lipid.

homologous phosphatidylcholines from sonicated vesicles to human erythrocytes and examined the transfer of one such lipid between two populations of human erythrocytes.

Materials and Methods

Blood was obtained as described previously (Ferrell et al., 1985). Lipids were purchased from Sigma [dilauroylphosphatidylcholine (DLPC),[1] dimyristoyl-PC (DMPC), dipalmitoyl-PC (DPPC), dipalmitoylphosphatidylglycerol (DPPG), egg lyso-PC (assayed by Sigma to contain 65% palmitoyl, 30% stearoyl, and 3% oleoyl chains), and cholesterol] and Avanti [DLPC, di(13:0)PC, and di(15:0)PC]. [^{14}C]DMPC was synthesized as described (Stockton et al., 1974); [^{14}C]lysopalmitoyl-PC ([^{14}C]lyso-PPC) and [^{3}H]-cholesteryl oleate were purchased from New England Nuclear. Egg lyso-PC micelles and small unilamellar PC vesicles were prepared as described in the preceding paper (Ferrell et al., 1985).

Cells were incubated with vesicles at 37 °C in capped plastic tubes at concentrations and for intervals specified under Results and in the figure legends. For incubations longer than 5 h, penicillin G (100 μg/mL) and tobramycin (40 μg/mL) were added. Two procedures were used to assess the transfer of lipids from vesicles to cells. For egg lyso-PC, DMPC, and DPPC, aliquots of cell–vesicle mixtures were placed on a cushion of 42% sucrose in NaCl/P_i (w/v) and separated by centrifugation for 3 min at 8800*g*. The amount of lipid transferred to the cells was determined from [^{14}C]lyso-PPC, [^{14}C]DMPC, or [^{14}C]DPPC in the cell pellet. Control experiments showed that the added radiolabel could be recovered quantitatively from the cell pellet plus supernatant. In some experiments, trace quantities of [^{3}H]cholesteryl oleate were used as a nontransferable vesicle marker. In one experiment, 3 mol % DPPG was cosonicated with DMPC to inhibit the possible formation of vesicle–cell complexes. For DLPC, di(13:0)PC, and di(15:0)PC, the amount of lipid transferred to cells was determined by assessing cell morphology by light microscopy and using the relationship between lipid incorporation and cell shape established in the preceding paper [Figure 7 in Ferrell et al. (1985)]. This procedure was rapid and reproducible and, for egg lyso-PC, DMPC, and DPPC, yielded results which agreed well with those obtained by using radiolabels.

Initial lipid transfer rates (v_o) were determined as a function of cell and vesicle concentrations. Rate coefficients were determined by nonlinear curve fitting of these data to eq 4 and 8 (see below) and also by graphic methods (see Table I). Within experimental error, the two procedures yielded indistinguishable results.

To assess intercell transfer of DLPC, red cells were incubated with 1 volume of 140 μM DLPC for 10 min at 37 °C. The DLPC-induced echinocytes were pelleted for 3 min at 8800*g*, washed twice with 2 volumes of NaCl/P_i, and reincubated with 1 volume of fresh (discocytic) erythrocytes and 2 volumes of NaCl/P_i. Cell morphology of the combined sample was monitored as a function of time.

Theory

Collision Models. In a one-step collision model, the rate of lipid transfer is first order in both vesicle and cell concentrations. If, however, lipid transfer involves the formation of a transient complex (Figure 1a,b), the kinetics become slightly more complicated.

Two versions of the transient collision model will be considered. The rate expressions for the two versions are algebraically identical, though the physical processes corresponding to the various rate coefficients are distinct and distinguishable. The first model is shown in Figure 1a. The donor and acceptor membranes collide to form a partially fused complex (McLean & Phillips, 1981). Transfer then involves lateral diffusion of lipids between the outer monolayers of the cell and vesicle membranes. In the second model (Figure 1b), the transient complex is more superficial, involving close apposition but not fusion of the donor and recipient membranes. Transfer then involves interbilayer translocation or flip-flop of lipids between the apposed membranes.

[1] Abbreviations: DLPC, dilauroylphosphatidylcholine; di(13:0)PC, ditridecanoylphosphatidylcholine; DMPC, dimyristoylphosphatidylcholine; di(15:0)PC, dipentadecanoylphosphatidylcholine; DPPC, dipalmitoylphosphatidylcholine; DPPG, dipalmitoylphosphatidylglycerol; lyso-PC, lysophosphatidylcholine; lyso-PPC, lysopalmitoylphosphatidylcholine; HCT, hematocrit; spin PC, 1-palmitoyl-2-[9-(4,4-dimethyloxazolidine-*N*-oxyl)stearoyl]phosphatidylcholine.

Table I: Predictions of the Transient Collision and Monomer Transfer Models

quantity	transient collision model	monomer transfer model
v_o	$v_o = \frac{k_1 k_2 L_{tot} C}{k_{-1} + k_2 + k_1(\sigma L_{tot} + C)}$	$v_o = \frac{k_1 k_2 L_{tot} C}{k_1 + k_{-1} L_{tot} + k_2 C}$
$\frac{1}{v_o}$	$\frac{1}{v_o} = \frac{k_{-1} + k_2}{k_1 k_2} \frac{1}{L_{tot}} \frac{1}{C} + \frac{\sigma}{k_2} \frac{1}{C} + \frac{1}{k_2 L_{tot}}$	$\frac{1}{v_o} = \frac{1}{k_2} \frac{1}{L_{tot}} \frac{1}{C} + \frac{k_{-1}}{k_1 k_2} \frac{1}{C} + \frac{1}{k_1} \frac{1}{L_{tot}}$
from $1/v_o$ vs. $1/C$ at fixed L_{tot}	slope $= \frac{k_{-1} + k_2}{k_1 k_2} \frac{1}{L_{tot}} + \frac{\sigma}{k_2}$	slope $= \frac{1}{k_2} \frac{1}{L_{tot}} + \frac{k_{-1}}{k_1 k_2}$
	intercept $= (1/k_2)(1/L_{tot})$	intercept $= (1/k_1)(1/L_{tot})$
	$v_{max} = k_2 L_{tot}$	$v_{max} = k_1 L_{tot}$
	$v_o = \frac{1}{2} v_{max}$ when $C = \frac{k_{-1} + k_2}{k_1} + \sigma L_{tot}$	$v_o = \frac{1}{2} v_{max}$ when $C = \frac{k_1}{k_2} + \frac{k_{-1}}{k_2} L_{tot}$
from $1/v_o$ vs. $1/L_{tot}$ at fixed C	slope $= \frac{k_{-1} + k_2}{k_1 k_2} \frac{1}{C} + \frac{1}{k_2}$	slope $= \frac{1}{k_2} \frac{1}{C} + \frac{1}{k_1}$
	intercept $= (\sigma/k_2)(1/C)$	intercept $= (k_{-1}/k_1 k_2)(1/C)$
	$v_{max} = (k_2/\sigma)C$	$v_{max} = (k_1 k_2/k_{-1})C$
	$v_o = \frac{1}{2} v_{max}$ when $L_{tot} = \frac{k_{-1} + k_2}{\sigma k_1} + \frac{1}{\sigma} C$	$v_o = \frac{1}{2} v_{max}$ when $L_{tot} = \frac{k_1}{k_{-1}} + \frac{k_2}{k_{-1}} C$

At early times when no lipid has yet been transferred, the rate of appearance of foreign lipid in the cells is

$$v_o = \frac{dL_c}{dt} = k_2 L_{cv} \quad (1)$$

where L_c is the concentration of cell-bound foreign lipid and L_{cv} represents foreign lipid in transient cell–vesicle complexes. All lipid concentrations in these derivations are expressed in moles per liter of supernatant. Assuming that the cell–vesicle complexes quickly reach a steady-state concentration, it follows that

$$\frac{dL_{cv}}{dt} = 0 = k_1 C_f L_v - (k_{-1} + k_2) L_{cv} \quad (2)$$

where L_v represents the vesicle lipid concentration and C_f represents the free surface area of the cells. This surface area can be expressed in the concentration units used for L_v and L_c. Taking the red cell volume to be 88 fL, the cell area to be 140 μm^2 (Wintrobe, 1981), the cross-sectional area per vesicle lipid to be 0.6 nm^2 (Cornell & Separovic, 1983), and the fraction of outer monolayer vesicle lipid to be 0.735, it follows that a suspension of cells at 1% HCT has the same surface area as a 60.12 μM suspension of vesicles.

At early times, the total lipid concentration $L_{tot} = L_v + L_{cv}$. The total cell surface area, C (again, expressed in concentration units for comparison to vesicle lipid concentrations as above), is the sum of the free cell surface area, C_f, and the area occupied by cell–vesicle complexes. This latter area is given by σL_{cv} where the constant σ is the ratio of cell area to vesicle area in each complex. If each cell–vesicle complex consists of a spherical vesicle of surface area $4\pi r^2$ occupying a circle of cell membrane whose area is πr^2, then $\sigma = 0.25$. Substituting $L_v = L_{tot} - L_{cv}$ and $C_f = C - \sigma L_{cv}$ into eq 2 and ignoring terms of order L_{cv}^2, it follows that

$$L_{cv} = \frac{k_1 L_{tot} C}{k_{-1} + k_2 + k_1(\sigma L_{tot} + C)} \quad (3)$$

$$v_o = \frac{k_1 k_2 L_{tot} C}{k_{-1} + k_2 + k_1(\sigma L_{tot} + C)} \quad (4)$$

The initial velocity v_o is first order in cell and vesicle concentrations (C and L_{tot}) only if $k_{-1} + k_2 \gg k_1(\sigma L_{tot} + C)$. Otherwise, at a given vesicle concentration, v_o is first order in C when C is small and zero order when C is large. Similarly, at a given cell concentration, v_o is first order in L_{tot} for small L_{tot} and zero order for large L_{tot}. This fact has not been appreciated by some critics of the collision model. Indeed, the collision model predicts that when $k_1 C \gg k_1 \sigma L_{tot} + k_{-1} + k_2$, lipid transfer will be first order in (donor) vesicle concentration and zero order in (acceptor) cell concentration, kinetic behavior previously considered to be the hallmark of monomer transfer.

Monomer Transfer Models. In the simplest monomer transfer model, the first step is the dissociation of a monomer of lipid (L_m) into the supernatant (Figure 1c). The lipid then collides with a cell and is incorporated into the cell membrane. At early times, the rate of appearance of foreign lipid in the cells is given by

$$v_o = \frac{dL_c}{dt} = k_2 C L_m \quad (5)$$

where, again, C represents the cell concentration and L_c the concentration of cell-bound foreign lipid. Under the steady-state assumption

$$\frac{dL_m}{dt} = 0 = k_1 L_v - (k_{-1} L_v + k_2 C) L_m \quad (6)$$

where L_v is the concentration of vesicle lipid. By substituting $L_v = L_{tot} - L_m$, ignoring terms of order L_m^2, and solving for L_m, it follows that

$$v_o = \frac{k_1 k_2 L_{tot} C}{k_1 + k_{-1} L_{tot} + k_2 C} \quad (7)$$

In the present work, we have used phospholipids at concentrations greatly in excess of their critical bilayer concentrations, which are defined by the ratio k_1/k_{-1} (Tanford, 1980; Nichols & Pagano, 1981). Thus, $k_1 \ll k_{-1} L_{tot}$, and we can simplify eq 7 to

$$v_o = \frac{k_1 k_2 L_{tot} C}{k_{-1} L_{tot} + k_2 C} \quad (8)$$

If $k_2 C \gg k_{-1} L_{tot}$, then v_o is first order in L_{tot} and zero order in C. Otherwise, v_o is saturable in both vesicle and cell concentrations, as was the case for collisional transfer (eq 4). Both

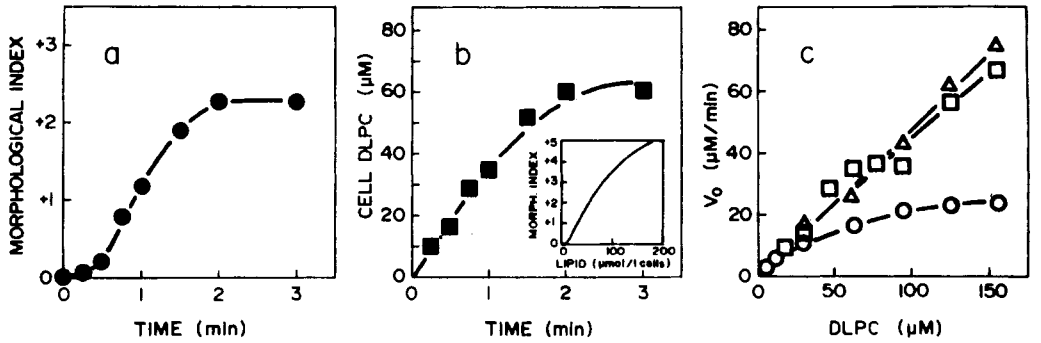

FIGURE 2: Transfer of DLPC from vesicles to cells. (a) Cell morphology as a function of time for erythrocytes incubated with 62.5 μmol of DLPC/L of supernatant at 50% hematocrit. (b) DLPC transferred to cells, calculated from the relationship between lipid incorporation and morphology (inset). (c) Initial rate of DLPC transfer as a function of vesicle concentration at (○) 10%, (□) 25%, and (△) 50% hematocrit.

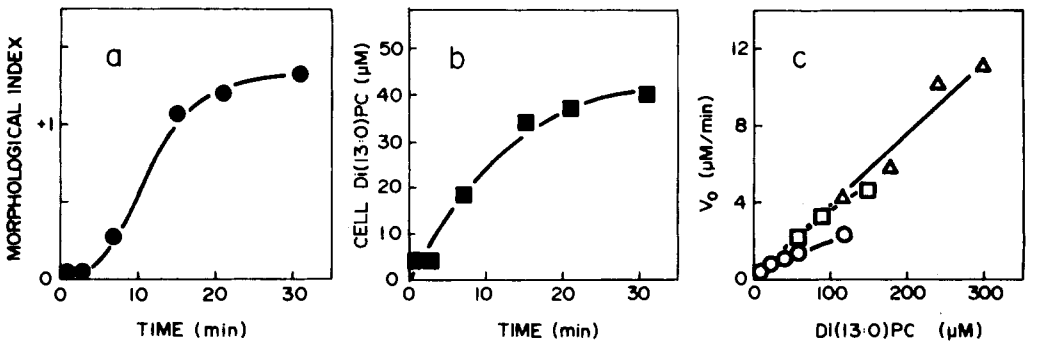

FIGURE 3: Transfer of di(13:0)PC from vesicles to cells. (a) Cell morphology as a function of time for erythrocytes incubated with 75 μmol of di(13:0)PC/L of supernatant at 50% hematocrit. (b) Di(13:0)PC transferred to cells, calculated from the relationship between lipid incorporation and morphology (see Figure 2b). (c) Initial rate of di(13:0)PC transfer as a function of vesicle concentration at (○) 10%, (□) 25%, and (△) 50% hematocrit.

models also predict that plotting $1/v_0$ vs. $1/L_{tot}$ for fixed values of C should yield families of straight lines whose intercepts vary with $1/C$. Similarly, plotting $1/v_0$ vs. $1/C$ for fixed values of L_{tot} should yield straight lines whose intercepts vary with $1/L_{tot}$. Table I summarizes these relationships.

RESULTS

DLPC. Erythrocytes were incubated at 10%, 25%, and 50% hematocrit with 5–155 μmol of DLPC/L of supernatant. The results of one such incubation are shown in Figure 2a,b. The cells quickly became echinocytic, reflecting the accumulation of DLPC in their membrane outer leaflets (Figure 2a). The incorporated DLPC was estimated from the relationship between cell morphology and lipid incorporation (inset, Figure 2b) determined in the preceding paper. After 3 min of incubation, all of the DLPC appeared to be incorporated into the cells (Figure 2b). The initial rate of transfer, v_0, was estimated from the early time points (t = 15, 30, and 45 s) and plotted as a function of DLPC concentration. As shown in Figure 2c, v_0 increased with both [DLPC] and hematocrit, as predicted by eq 4 and 8. Double-reciprocal plots of the data in Figure 2c yielded parallel lines (not shown).

Di(13:0)PC. Erythrocytes were incubated at 10%, 25%, and 50% hematocrit with 10–300 μM di(13:0)PC. Di(13:0)PC transferred more slowly and less extensively than DLPC. Lipid transfer appeared to be complete within about 30 min, with 50–70% of the lipid incorporated into the cells (Figure 3a,b). The initial rate of lipid transfer increased with both hematocrit and vesicle concentration (Figure 3c) and was saturable in both. Again, double-reciprocal plots yielded parallel lines (not shown).

DMPC. Three concentrations of erythrocytes (hematocrits of 10%, 25%, and 50%) were incubated with DMPC vesicles (14–144 μmol/L of supernatant), and the amount of vesicle lipid associated with the cells was measured as a function of time (Figure 4a,b). The initial rate of lipid transfer (v_0) increased with both vesicle and cell concentrations in a saturable fashion (Figure 4c,d). Plots of $1/v_0$ vs. $1/C$ or $1/L_{tot}$ yielded straight lines (Figure 4e,f); however, the slopes of the lines were not identical, as was the case for DLPC and di(13:0)PC. Plots of the slopes and intercepts of the lines vs. $1/C$ or $1/L_{tot}$ yielded straight lines (Figure 4e,f, insets). DMPC transfer was unaltered by adding 3% DPPG to the DMPC vesicles (data not shown).

Di(15:0)PC. Erythrocytes (hematocrits of 20% and 50%) were incubated with di(15:0)PC at concentrations from 0.3 to 6.9 mM. Crenation occurred on a time scale of several hours (Figure 5a) and reached a plateau after less than 5% of the vesicle lipid was associated with the cells (Figure 5b). Lipid transfer was a saturable function of hematocrit and vesicle concentration (Figure 5c), and plots of $1/v_0$ vs. $1/L_{tot}$ yielded straight lines with different slopes.

DPPC. DPPC transfer was slow and difficult to quantify. Erythrocytes appeared to take up substantial amounts of [^{14}C]DPPC from DPPC vesicles (Figure 6). However, the nontransferable lipid marker [^{3}H]cholesteryl oleate also appeared to be taken up by the cell. When cells treated with [^{14}C]DPPC/[^{3}H]cholesteryl oleate vesicles were washed and reincubated with unlabeled DPPC vesicles, the cells rapidly lost 75% of the lipid markers to the supernatant (Figure 6). In contrast, DMPC exchanges out of cells at a rate comparable to its rate of dissociation from vesicles (Ferrell et al., 1985). The rapid dissociation of cell-associated DPPC suggests that most of it was only loosely bound, not intercalated in the membrane. This conclusion is consistent with the observation that erythrocytes incubated with DPPC do not crenate, even after 20-h incubation with a high concentration of DPPC (20 mM) and low hematocrit (10%). Instead, the cells become

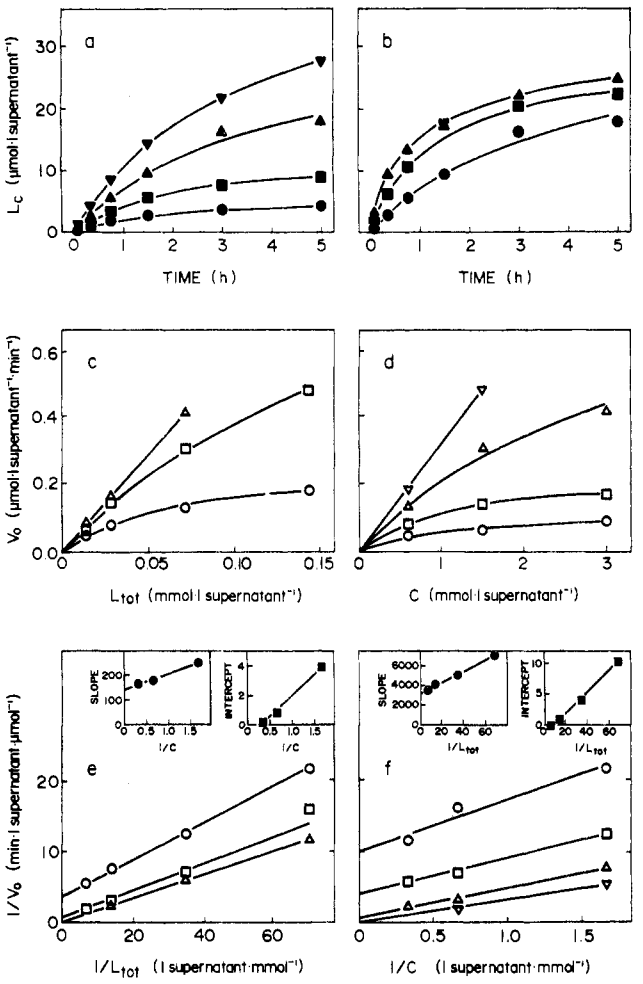

FIGURE 4: DMPC transfer from vesicles to cells. (a) Cell DMPC as a function of time for cells incubated at constant hematocrit (10% hematocrit, equivalent to C = 0.60 mmol/L of supernatant) and four vesicle concentrations: (●) 0.014 mmol/L of supernatant; (■) 0.029 mmol/L of supernatant; (▲) 0.072 mmol/L of supernatant; (▼) 0.144 mmol/L of supernatant. (b) Cell DMPC as a function of time for cells incubated at constant vesicle concentration (L_{tot} = 0.072 mmol/L of supernatant) and three hematocrits: (●) 10% hematocrit or 0.60 mmol/L of supernatant; (■) 25% hematocrit or 1.5 mmol/L of supernatant; (▲) 50% hematocrit or 3.0 mmol/L of supernatant. (c) Initial rate of lipid transfer, v_o, as a function of vesicle concentration at three hematocrits: (○) 10% hematocrit or 0.6 mmol/L of supernatant; (□) 25% hematocrit or 1.5 mmol/L of supernatant; (△) 50% hematocrit or 3.0 mmol/L of supernatant. (d) Initial rate of lipid transfer, v_o, as a function of hematocrit at four vesicle concentrations: (○) 0.014 mmol/L of supernatant; (□) 0.029 mmol/L of supernatant; (△) 0.072 mmol/L of supernatant; (▽) 0.144 mmol/L of supernatant. (e) Double-reciprocal plots of the data in (c). Insets show the slopes (in minutes) and intercepts (in minutes liters of supernatant per micromole) as a function of $1/C$ (in liters of supernatant per millimole). (f) Double-reciprocal plots of the data in (d). Insets show the slopes (in minutes) and intercepts (in minutes liters of supernatant per micromole) as a function of $1/L_{tot}$ (in liters of supernatant per millimole).

slightly cupped, reflecting the fact that cholesterol transfer from the cells to the vesicles is more rapid than DPPC transfer from vesicles to cells.

Other Lipids. Egg lyso-PC transfer was rapid, with a half-time of less than 7 s. Spin PC transfer appeared to occur on a time scale comparable to DMPC.

Effect of Donor Membrane Phase State. Trace amounts of [^{14}C]DMPC were cosonicated with DMPC or DPPC, and the resulting vesicles were incubated with cells. At the temperature chosen (37 °C), DMPC vesicles are fluid, and DPPC vesicles are near the bottom of their melting range (Cook et al., 1980). As is shown in Figure 7, erythrocytes took up [^{14}C]DMPC at approximately equal rates from the two types of vesicles.

Intercell Transfer of DLPC. Red cells were incubated with 1 volume of 140 μM DLPC to yield a nearly uniform sample of stage 3 echinocytes. These echinocytes were washed and resuspended in buffer with 1 volume of untreated discocytes. As shown in Figure 8, initially there were two distinct populations of cells: stage 0 discocytes and stage 3 echinocytes. Within 20 min, these populations had merged to become a single population of stage 1 and 2 echinocytes. The half-time of this process was 7 ± 3 min (average of three experiments).

Discussion

For each phosphatidylcholine studied, the rate of lipid transfer between vesicles and erythrocytes depended on both the cell and vesicle concentrations. As predicted by both the collision and monomer transfer models, v_{max} was proportional to the hematocrit at fixed vesicle concentration and proportional to vesicle concentration at fixed hematocrit. The order of the reaction does not distinguish between the two models.

The data from Figures 2–5 were used to calculate rate coefficients for transfer of each lipid species according to both the collision and monomer transfer models (eq 4 and 8). For DPPC transfer, a range of rates was estimated by assuming that at most 50% (based on the binding of [^{3}H]cholesteryl oleate and [^{14}C]DPPC) and at least 12% (based on the amount of the two markers left after 1-h incubation with unlabeled DPPC) of the lipid–cell association reflected true lipid transfer. These rate coefficients are shown in Table II and, together with the experiment summarized in Figure 8, provide a basis for testing the collision and monomer transfer models.

Collision Models. The rate data yield a physically unreasonable value for σ, the constant relating the amount of cell and vesicle area occluded by contact in each transient cell–vesicle complex. In deriving eq 4, it was argued above that σ should be roughly 0.25, meaning that each complex would remove 1 unit of cell area for each 4 units of vesicle area. However, from the rate data for DMPC, σ was calculated to be about 15. In other words, the collision models predict that lipid transfer can be saturated more easily by raising C than by raising L_{tot}; the opposite is observed. It is possible to reconcile this observation with the collision models by assuming that only a small fraction (roughly 2%) of the cell surface area can participate in productive collisions, but we know of no other evidence supporting this assumption. Thus, the data for DMPC transfer can be reconciled, though with some difficulty, with the collision models. The rate coefficients for each of the other lipids taken individually can be rationalized similarly with both collision models.

The relationship between acyl chain length and lipid transfer rates (Figure 9), which will be discussed further below, rules out the transient collision mechanism shown in Figure 1a. The rate coefficient k_2, which represents the rate of lateral diffusion of lipid within the cell–vesicle complex, is found to decrease exponentially with increasing acyl chain length. As pointed out by McLean & Phillips (1981), the rate of lateral diffusion should be similar for all of the lipids studied, including the "nontransferable" lipid cholesteryl oleate. In the more superficial transient collision model (Figure 1b), k_2 represents interbilayer translocation of lipid molecules. Interbilayer flip-flop involves the entropically unfavorable passage of hydrophobic acyl chains through the hydrophilic head-group region. This step is energetically analogous to the dissociation of a monomer from a vesicle, and the rate of this step might decrease exponentially with increasing acyl chain length. It

Table II: Rate Coefficients for Lipid Transfer

collision: monomer:	k_2 k_1 (min^{-1})	σ k_{-1}/k_2	$(k_{-1} + k_2)k_1$ (M)[a]	k_1/k_{-1} (M)[a]	k_{-1} (min^{-1} M^{-1})[a]	k_2 (min^{-1} M^{-1})[a]
DLPC	$(5.6 \pm 1.5) \times 10^{-1}$	4.7 ± 3.4	0	3.4×10^{-7} [b]	$(1.5 \pm 0.4) \times 10^{6}$	$(4.1 \pm 2.3) \times 10^{5}$
di(13:0)PC	$(4.0 \pm 0.7) \times 10^{-2}$	5.7 ± 4.2	0	6.6×10^{-8} [b]	$(6.0 \pm 1.1) \times 10^{5}$	$(1.5 \pm 1.3) \times 10^{4}$
DMPC	$(9.3 \pm 3.9) \times 10^{-3}$	15.1 ± 5.6	$(5.8 \pm 2.4) \times 10^{-4}$	1.3×10^{-8} [b]	$(7.1 \pm 3.0) \times 10^{5}$	$(5.5 \pm 4.0) \times 10^{4}$
di(15:0)PC	$(2.2 \pm 1.5) \times 10^{-4}$	[c]	[c]	2.4×10^{-9} [b]	$(9.2 \pm 6.3) \times 10^{4}$	[c]
DPPC	$(0.3\text{–}2.7) \times 10^{-4}$ [d]	[c]	[c]	4.7×10^{-10} [e]	$(0.7\text{–}5.7) \times 10^{5}$	[c]
spin PC	$(3.0 \pm 1.0) \times 10^{-3}$	[c]	[c]	[c]	[c]	[c]
egg lyso-PC	>6	[c]	[c]	7×10^{-6} [f]	$>9 \times 10^{5}$	[c]

[a] Molar units are taken to mean moles per liter of supernatant. [b] Interpolated from critical micelle/bilayer concentrations reported for diheptanoyl-PC, dioctanoyl-PC, didecanoyl-PC, and DPPC [summarized in Tanford (1980)]. [c] Insuffient data. [d] Range calculated as described in the text. Other ranges denote standard deviations. [e] Reported by Smith & Tanford (1972). [f] Reported by Haberland & Reynolds (1975).

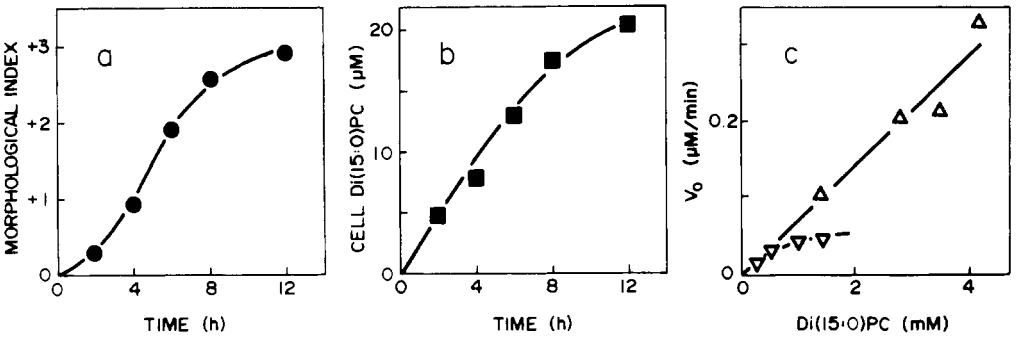

FIGURE 5: Transfer of di(15:0)PC from vesicles to cells. (a) Cell morphology as a function of time for erythrocytes incubated with 830 μmol of di(15:0)PC/L of supernatant at 20% hematocrit. (b) Di(15:0)PC transferred to cells, calculated from the relationship between lipid incorporation and morphology (see Figure 2b). (c) Initial rate of di(15:0)PC transfer as a function of vesicle concentration at (▽) 20% and (△) 50% hematocrit.

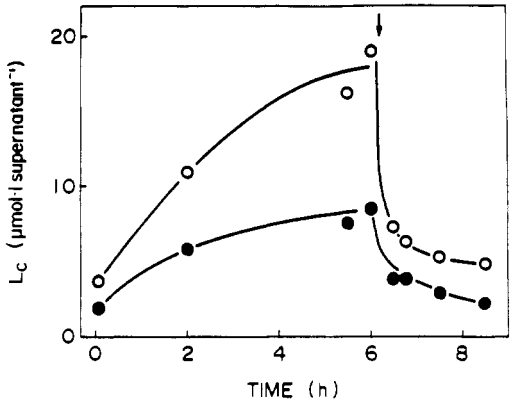

FIGURE 6: DPPC transfer from vesicles (0.133 mmol/L of supernatant) to cells (50% hematocrit) as monitored by [^{14}C]DPPC (○) and corrected for [^{3}H]cholesteryl oleate binding (●). After 6-h incubation, aliquots of the cells were centrifuged, washed once in 4 volumes of NaCl/P_i, and incubated beginning at t = 6 h 15 min with an equal volume of unlabeled DPPC vesicles (26.6 mmol/L of supernatant).

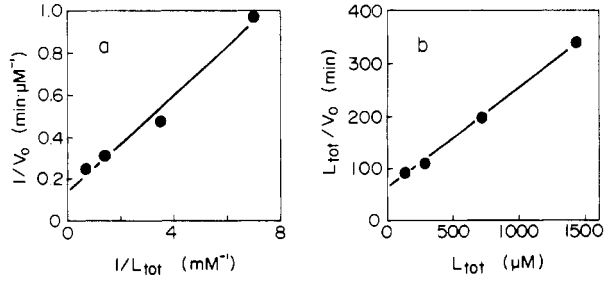

FIGURE 7: [^{14}C]DMPC transfer from DMPC (a) and DPPC (b) vesicles. Initial velocities are plotted in accordance with eq 8 (a) and eq 12 from the preceding paper (b) (Ferrell et al., 1985), both based on monomer transfer models. The rate of monomer dissociation from donor vesicles is calculated to be 9×10^{-3} min^{-1} for (a) (taken as 1/slope) and 17×10^{-3} min^{-1} for (b) (taken as 1/intercept).

is therefore possible to rationalize the observed acyl chain length dependence of this rate coefficient with the transient

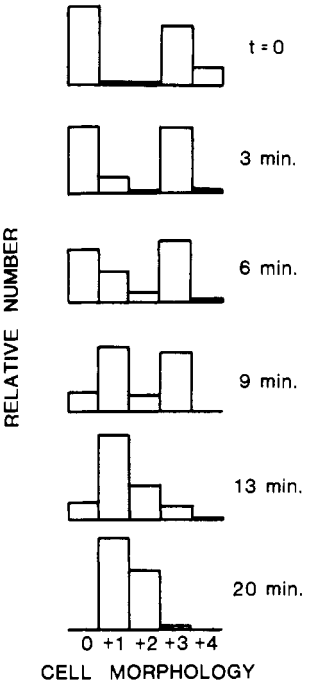

FIGURE 8: Transfer of DLPC between red cells. DLPC-induced echinocytes were mixed with DLPC-free discocytes at t = 0. By 20 min, the cells assumed intermediate morphologies consistent with equilibration of the DLPC among the cells.

collision model shown in Figure 1b, but not the partial fusion model shown in Figure 1a.

The observation of rapid intercell transfer of DLPC (Figure 8) is inconsistent with both collision models. Because of the relatively large mass of cells, the frequency of cell–cell collisions should be small compared to cell–vesicle collisions. In addition, close apposition of lipid portions of the two cell membranes should be severely hindered by steric effects of proteins and repulsive Coulombic interactions. Thus, the transient collision models predict that intercell transfer of

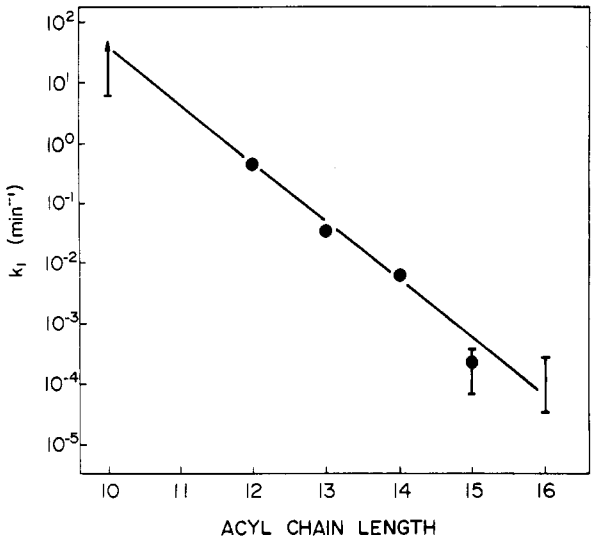

FIGURE 9: Rate of monomer dissociation (k_1) as a function of acyl chain length for diacyl-PC. Data points represent the measured dissociation rates for DLPC, di(13:0)PC, DMPC, and di(15:0)PC; a range of rate coefficients for DPPC estimated as described under Discussion; and the measured lower bound for the egg lyso-PC dissociation coefficient. The latter phospholipid is approximately equal to didecanoyl-PC in hydrophobicity, and its rate coefficient is plotted accordingly.

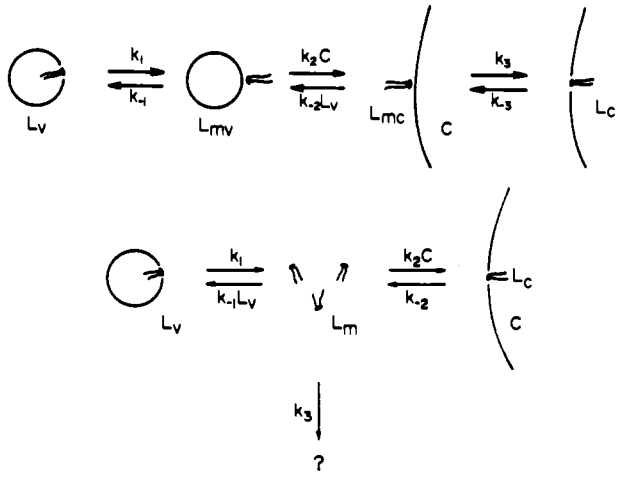

FIGURE 10: Two possible modifications of the monomer transfer model: top, "caged" monomer transfer; bottom, an additional reaction pathway for lipid monomers. The expressions for v_o as a function of C and L_{tot} are

$$v_o = \frac{k_1k_2k_3L_{tot}C}{k_{-1}k_3 + k_{-1}k_{-2}L_{tot} + k_2k_3C} \quad (9)$$

$$v_o = \frac{k_1k_2L_{tot}C}{k_3 + k_{-1}L_{tot} + k_2C} \quad (10)$$

phospholipids should be much slower than cell–vesicle transfer. As shown in Figure 8, intercell transfer of DLPC is only slightly slower than vesicle–cell transfer (characteristic times of roughly 7 and 1 min, respectively). This slowing probably reflects the relative ease of monomer dissociation (see below) from strained, highly curved vesicles; as shown in the previous paper (Ferrell et al., 1985), the dissociation of DMPC from cells is also about 7-fold slower than the dissociation of DMPC from vesicles. The collision models are also difficult to reconcile with the observation that DPPG, an acidic phospholipid that inhibits PC vesicle fusion and might be expected to prevent close contact between vesicles and negatively charged cells, does not alter the kinetics of DMPC transfer between vesicles and cells.

In summary, the transient collision models cannot be ruled out on the basis of reaction order; as predicted, the rate of lipid transfer increases in a saturable fashion with increasing cell and vesicle concentrations. The rate coefficients for DMPC transfer imply that if a transient collision model were operating, only a small percentage of the cell surface area could be available for productive collisions. The dramatic dependence of k_2 on acyl chain length is inconsistent with the collision/lateral diffusion mechanism (Figure 1a) but is consistent with the collision/interbilayer flip-flop mechanism (Figure 1b). However, neither transient collision model can be easily reconciled with the observation of rapid intercell transfer of DLPC.

Monomer Transfer Models. The relative magnitudes of k_{-1} and k_2 (whose ratio corresponds to σ in the collision models) are compatible with the monomer transfer model. As shown in Table II, the rate coefficient for uptake of a monomer by a vesicle (k_{-1}) was larger than that for uptake by a cell (k_2). This observation might reflect the relative ease of inserting a monomer into the highly curved vesicle membrane.

The dependence of lipid transfer on acyl chain length implies that the free energy of activation for lipid transfer increases linearly with increasing acyl chain length, as predicted by the monomer transfer model. At constant cell and vesicle concentrations, the rate of lipid transfer decreased exponentially as the acyl chain length increased. One rate coefficient (corresponding to k_1 in the monomer transfer model and k_2 in the collision model) could largely account for this dramatic decrease. The value of this rate coefficient decreased exponentially with increasing acyl chain length, as predicted by the monomer transfer model (Figure 9). Addition of one carbon to each PC acyl chain resulted in about a 9-fold decrease in k_1. This relationship held over a wide range of characteristic times and provides strong circumstantial support for the monomer transfer model.

Egg lyso-PC is less hydrophobic than the diacyl-PC's employed. The monomer transfer model predicts that it should therefore transfer more rapidly than the other phospholipids, as was observed (Table II). Measurements of critical micelle concentrations suggest that lyso-PPC (Haberland & Reynolds, 1975) and didecanoylphosphatidylcholine (Reynolds et al., 1977) have similar monomer dissociation rates. The value of k_1 extrapolated for lyso-PPC and didecanoylphosphatidylcholine is about 40 min^{-1} (Figure 9), compatible with our experimentally determined lower bound of 6 min^{-1}.

The data in Figure 7 suggest that the phase state of the donor membrane is significantly less important than the acyl chain length of the lipid in determining lipid transfer rates. This suggests that the free energy of monomer dissociation arises more from the monomer–aqueous phase interaction than from the membrane defect caused by the loss of a monomer. DMPC transfer from DPPC vesicles obeys the kinetic equation derived in the preceding paper for monomer transfer between "inert" membranes.

Inconsistencies between the monomer transfer model and the observed kinetics were found only for the slowly transferred lipids DMPC and di(15:0)PC. According to eq 8, double-reciprocal plots should have yielded parallel lines; however, the observed slopes of these lines varied systematically with $1/L_{tot}$ or 1/hematocrit (Figure 4e,f, insets). This finding suggests that the actual transfer mechanism for these species is more complicated than that shown in Figure 1c. Two plausible modifications of the monomer transfer model are shown in Figure 10. In the first, lipid transfer can occur between lipid monomers that have not yet escaped the unstirred aqueous phase near the vesicle. In the second, lipid monomers

are assumed to undergo some process other than collisions with vesicles or cells. Both models predict the nonparallel slopes found in the double-reciprocal plots, and both predict that the monomer dissociation rate can be deduced by extrapolating the slope of $1/v_o$ vs. $1/L_{tot}$ to infinite hematocrit (Table I). We have no basis for discriminating between these models or other possible models yielding similar kinetic predictions (provided that such models include a monomer transfer step). The discrepancies could also possibly result from experimental complications such as the concomitant transfer of cholesterol from cells to vesicles, which occurs to a significant extent on the time scale of DMPC and di(15:0)PC transfer and is difficult to accommodate in theoretical models.

Spin-labeled PC dissociated from vesicles on about the same time scale as DMPC, with $k_1 = (3.0 \pm 1.0) \times 10^{-3}$ min^{-1} (Table II). The similarity between these rate coefficients probably reflects a balance between the hydrophobicity of spin PC's longer acyl chains (C_{16} and C_{18} vs. C_{14}) and the hydrophilicity of its oxazolidine ring.

Some insight into the behavior of natural membranes can be gleaned from the data in Table II and Figure 9. Natural phosphatidylcholines almost always possess 16 or more carbons in each acyl chain. Their spontaneous transfer between membranes would therefore be expected to occur on time scales of weeks to years. Less polar phospholipids might exchange even more slowly. This would suggest that it is advantageous for natural membranes to adjust their fluidity by adding unsaturations to long-chain fatty acids instead of the energetically more economical route of decreasing the chain length; long-chain lipids ensure the integrity of the membrane.

ACKNOWLEDGMENTS

We thank Gerald Keep for suggesting the idea of "caged" monomer transfer and Alexandra Newton for help with nonlinear curve fitting.

Registry No. DLPC, 18285-71-7; di(13:0)PC, 75340-69-1; DMPC, 13699-48-4; di(15:0)PC, 67896-63-3; DPPC, 2644-64-6; 1-palmitoyl-2-stearoylphosphatidylcholine, 10589-47-6.

REFERENCES

Backer, J. M., & Dawidowicz, E. A. (1981) *Biochemistry 20*, 3805–3810.

Cook, S. L., Bouma, S. R., & Huestis, W. H. (1980) *Biochemistry 19*, 4601–4607.

Cornell, B. A., & Separovic, F. (1983) *Biochim. Biophys. Acta 733*, 189–193.

DeCuyper, M., Joniau, M., & Dangreau, H. (1983) *Biochemistry 22*, 415–420.

Devaux, P., Scandella, C. J., & McConnell, H. M. (1973) *J. Magn. Reson. 9*, 474–485.

Duckwitz-Peterlein, G., Eilenberger, G., & Overath, P. (1977) *Biochim. Biophys. Acta 469*, 311–325.

Ferrell, J. E., Jr., Lee, K.-J., & Huestis, W. H. (1985) *Biochemistry* (preceding paper in this issue).

Haberland, M. E., & Reynolds, J. A. (1975) *J. Biol. Chem. 250*, 6636–6639.

Kremer, J. M. H., Kops-Werkhoven, M. M., Pathmamanoharan, C., Gijzeman, O. L. J., & Wiersema, P. H. (1977) *Biochim. Biophys. Acta 448*, 245–264.

Lange, Y., Molinaro, A. L., Chauncey, T. R., & Steck, T. L. (1983) *J. Biol. Chem. 258*, 6920–6926.

March, J. (1977) in *Advanced Organic Chemistry*, 2nd ed., pp 194–195, McGraw-Hill, New York.

Martin, F. J., & MacDonald, R. C. (1976) *Biochemistry 15*, 321–327.

Massey, J. B., Gotto, A. M., & Pownall, H. J. (1982) *J. Biol. Chem. 257*, 5444–5448.

McLean, L. R., & Phillips, M. C. (1981) *Biochemistry 20*, 2893–2900.

Nichols, J. W., & Pagano, R. E. (1981) *Biochemistry 20*, 2783–2789.

Reynolds, J. A., Tanford, C., & Stone, W. L. (1977) *Proc. Natl. Acad. Sci. U.S.A. 74*, 3796–3799.

Roseman, M. A., & Thompson, T. E. (1980) *Biochemistry 19*, 439–444.

Smith, R., & Tanford, C. (1972) *J. Mol. Biol. 67*, 75–83.

Stockton, G. W., Polnaszek, C. F., Leitch, L. C., Tulloch, A. P., & Smith, I. C. P. (1974) *Biochem. Biophys. Res. Commun. 60*, 844–850.

Tanford, C. (1980) in *The Hydrophobic Effect*, 2nd ed., Wiley, New York.

Wintrobe, M. M. (1981) in *Clinical Hematology*, 8th ed., Lea & Febiger, Philadelphia, PA.